



Research Article

The Discrete Load Frequency Control System Using a Robust Periodic Output Feedback Controller

Hukam Chand Kumawat,¹ Mahendra Bhadu,¹ Arvind Kumar,¹ Om Prakash Mahela ,^{2,3}
Baseem Khan ,^{3,4} Divya Anand,^{5,6} and Jose Breñosa^{7,8}

¹Department of Electrical Engineering, Government Engineering College Bikaner, Rajasthan, India

²Power System Planning Division, Rajasthan Rajya Vidyut Prasaran Nigam Ltd, Jaipur-302005, India

³Engineering Research and Innovation Group (ERIG), Universidad Internacional Iberoamericana, Campeche, C. P. 24560, Mexico

⁴Department of Electrical and Computer Engineering, Hawassa University, Awasa, Ethiopia

⁵School of Computer Science and Engineering, Lovely Professional University, Punjab-144411, India

⁶Higher Polytechnic School, Universidad Europeadel Atlántico, C/Isabel Torres 21,39011, Santander, Spain

⁷Department of Project Management, Universidad Internacional Iberoamericana, Campeche 24560, Mexico

⁸Department of Project Management, Universidad Internacional Iberoamericana, Arecibo 00613, Puerto Rico, USA

Correspondence should be addressed to Baseem Khan; baseem.khan1987@gmail.com

Received 9 August 2022; Revised 24 March 2023; Accepted 30 March 2023; Published 17 April 2023

Academic Editor: Bhargav Appasani

Copyright © 2023 Hukam Chand Kumawat et al. This is an open access article distributed under the Creative Commons Attribution License, which permits unrestricted use, distribution, and reproduction in any medium, provided the original work is properly cited.

The load frequency control (LFC) is a most important tool for the frequency regulation mechanism in the widely spread modern power system. The LFC system consists of a communication structure to transmit the measurement and control signal. Usually the controllers in LFC systems are designed and implemented in continuous mode of operation. This article investigates the discrete mode load frequency control (LFC) mechanism, by employing the concept of the periodic output feedback (POF)-based controller with varying input and output sampling frequencies. Both the optimal sampling frequency and the optimal POF controller gain matrix are found by using the particle swarm optimization (PSO) method. The POF-based controller is intended for usage in two-area multisource LFC systems, with varying input and output sampling frequencies. The performance analysis takes into account a variety of scenarios, including those without a conventional stabilizer, with conventional continuous and corresponding discrete mode PSS, and a proposed discrete mode POF controller. Furthermore, the efficacy of the discrete mode POF controller is evaluated on the MATLAB/Simulink platform.

1. Introduction

1.1. Background. Numerous control strategies have been considered, and LFC has been the focus of research in power system studies for more than 40 years. It is thought that by systematically incorporating some of the existing control schemes into LFC operation and extracting their best aspects, a significantly better performance can be attained. The main functions of LFC in power systems are as follows: (1) maintaining zero steady-state errors for frequency deviations, (2) preventing sudden load disturbances, (3)

minimizing unscheduled tie-line power flows between neighboring areas and transient variations in area frequency, (4) dealing with modeling uncertainties and system nonlinearities within a tolerable region, and (5) ensuring ability to perform well under prescribed overshoot and setting time in frequency and tie-line power deviation [1, 2].

1.2. Literature Review. The sampled tie-line power and frequency measurements are transmitted to controller location via a communication channel. To handle the discrete

sampled signal, the controller needs to be implemented and executed in the discrete domain. The majority of past work in the LFC domain has focused on an interconnected thermal system, with the multiarea multisource hydrothermal system having continuous mode controllers [3–5].

However, in the research on discrete two-time scale systems [6–8] and singularly perturbed discrete systems [9–11], the subject of output feedback design has received minimal attention. The pole assignment problem for linear discrete-time systems by periodic output-feedbacks has been considered in [12–14]. The pole placement problem is to consider the potential of time varying fast output sampling feedback, with the fast output sampling approach proposed by Werner and Furuta [15]. The static output feedback problem is one of the most investigated problems in the control theory and application [16, 17]. Output feedback can be realized by using the fast output sampling (FOS) technique [18] or by periodic output feedback [19]. Load frequency control (LFC) of interconnected power systems integrated with conventional, renewable, and sustainable energy sources. The objective of LFC is to quickly stabilize the deviations in frequency and tie-line power following load fluctuations [20–24].

1.3. Research Gap and Motivation. Many researchers, on the other hand, have employed optimum control techniques to develop the controllers. These techniques create a gain matrix that may be applied to state feedback control by using the state-space representation of a power system model. For constructing a PSS based on output feedback, dynamic output feedback techniques are used [25, 26]. Closed loop stability and complete pole assignment are not guaranteed by the static output feedback approach. However, the discrete mode controllers with varying sampling frequencies in the LFC system still need attention and need to be explored further. The addition of renewable energy sources further may increase the complexity in the given scenario.

1.4. Challenges. The pole placement problem can be solved by time varying POF, as shown by Chammas and Leondes [27] because the discrete time system poles can be allocated by periodic time-changing piecewise constant output feedback if the plant is controllable and observable. An approach for designing a POF controller for a singularly perturbed discrete system that does not require the system's states for feedback was proposed in [28]. A significant amount of the study has been conducted in the subject of designing local PSSs in power systems using the POF technique in the recent past [29]. The POF technique has not yet been applied to obtain an optimal sampling rate in the LFC system, to the best of the authors' knowledge. Furthermore, the POF-based control system works with the varying sampling frequencies. The optimal input-output sampling frequency needs to be optimal for overall stability enhancement.

1.5. Contribution

- (i) The main purpose of this article is to suggest the best input-output sampling time intervals out of different data reporting rates for the discrete mode controller in a given LFC system. The controller is designed to account for the fact that a data reporting rate can only change in a set range [30].
- (ii) An improved squirrel search algorithm driven cascaded 2DOF-PID-FOI controller for load frequency control of the renewable energy-based hybrid power system is presented in [31–33]. Hybrid gravitational–firefly algorithm-based load frequency control for the hydrothermal two-area system is presented in [34]. Load frequency control using the hybrid intelligent optimization technique [35], the PI controllers, and its optimal tuning for load frequency control are described in [36–38]. Automatic generation control for the hybrid hydrothermal system using soft computing techniques is presented in [39]. An improved particle swarm optimization technique and its application in load frequency control are presented in [40].
- (iii) As a consequence, two output sample frequencies of 25 and 12.5 Hz with sampling intervals of 0.04 and 0.08 sec each are examined. To show the control design exercise, a time delay of 0.1 sec in feedback signal is considered in this article. The corresponding representation of time delay is executed using its third order of the Pade approximation method. The efficacy of the proposed discrete mode controller embedded in the LFC system is verified on the actual nonlinear Simulink model in the MATLAB/Simulink platform.

1.6. Paper Organization. The rest of this article is structured as follows: The background of POF control is presented in Section 2. The case studies in Section 3 offer an overview of the test system as well as the time delay in the feedback signal. In Section 4, the brief theory regarding control strategies such as conventional PSS and POF controller has been discussed. Section 5 contains the simulation result analysis and discussion. Finally, this article concludes with a list of references in Section 6.

2. Background OF POF Control

The following is a representation of the continuous mode time invariant n^{th} order linear system's state-space model:

$$\begin{aligned}\dot{x} &= Ax + Bu, \\ y &= Cx,\end{aligned}\tag{1}$$

when sampled at τ second, the continuous time system discussed above yields a discrete time model.

$$\begin{aligned} x((k+1)\tau) &= \phi_\tau x(k) + \Gamma_\tau u(k), \\ y(k) &= Cx(k), \end{aligned} \quad (2)$$

where, $x \in R^n$, $u \in R^n$, $y \in R^n$, Γ_τ , ϕ_τ , ϕ , Γ , and C are constant matrices of appropriate dimensions.

$x = [x_1^T, \Delta P_{ei} \dots \dots, x_{N-1}^T, \Delta P_{e(N-1)} \dots \dots, x_N^T]^T$; $n = \sum_i n_i$ $(N-1)$ n -state vector, $u = [u_1 \dots \dots u_N]^T = [\Delta P_{Di} \dots \dots \Delta P_{DN}]^T$ n -control input vector; $d = [d_1 \dots \dots, d_N]^T = [\Delta P_{Di} \dots \dots \Delta P_{DN}]^T$ n -disturbance input vector; and $v = [v_1 \dots \dots, v_N]^T$ $2N$ -measurable output vector. A , B , Γ , C , H are, in order, system, control, disturbance, output distribution, and the matrix of the measurable output distribution, respectively.

For any given number N , which may be more than or equal to the system's controllability index and $\Delta = \tau/N$, the system of (1) can be resampled at Δ seconds. Hence equation (1) can be written as follows:

$$x(k+1) = \phi x(k) + \Gamma u(k), \quad (3)$$

$$y(k) = Cx(k). \quad (4)$$

In this case, x , u , and y are Rn , whereas ϕ_τ , Γ_τ , ϕ , Γ , and C are constant matrices with the specified dimensions. The system's output is sampled at intervals of time $t = k\tau$, where $k = 0, 1, 2, \dots$. When assuming that the hold function is constant, the N subintervals with fixed length $\Delta = \tau/N$ are used. The control law thereby has a new significance.

$$u(t) = K_l y(k\tau), \quad (5)$$

$$k\tau + l\Delta \leq t < k\tau + (l+1)\Delta, \quad (6)$$

$$K_{l+N} = K_l, \{for\ l = 0, 1, \dots, (N-1)\}, \quad (7)$$

An output feedback gain $K(t)$, time varying in nature, is obtained for $0 \leq t < \tau$ when N gains $\{K_0, K_1, \dots, K_{N-1}\}$ are placed in (7). In this situation, it is worth to mention that (ϕ_τ, C) and (ϕ, Γ) are observable and controllable, respectively. Now, defining

$$K = \begin{bmatrix} K_0 \\ K_1 \\ \vdots \\ K_{N-1} \end{bmatrix}; u(k\tau) = Ky(k\tau) = \begin{bmatrix} u(k\tau) \\ u(k\tau + \Delta) \\ \vdots \\ u(k\tau + \tau - \Delta) \end{bmatrix}. \quad (8)$$

In (4), the system is subjected to the control law, yielding

$$x((k+1)\tau) = \phi x(k\tau) + \Gamma Ky(k\tau), \quad (9)$$

and using equations (8) and (9), it becomes

$$x((k+1)\tau) = (\phi + \Gamma KC)x(k\tau). \quad (10)$$

Similarly, in equation (2), applying the control law to the system yields

$$x((k+1)\tau) = \phi^N x(k\tau) + \Gamma u(k\tau). \quad (11)$$

Hence, the closed-loop τ system results into

$$x((k+1)\tau) = (\phi^N + \Gamma KC)x(k\tau), \quad (12)$$

$$\text{Here } \Gamma = [\phi^{N-1}\Gamma \dots \Gamma]. \quad (13)$$

G is considered as an output injection gain matrix, while maintaining $(\phi^N + GC)$ in stable condition. The G can be obtained as follows:

$$\rho(\phi^N + GC) < 1. \quad (14)$$

Here, $\rho()$ denotes the spectral radius. Hence, POF gain K is obtained as [26] follows:

$$\Gamma K = G. \quad (15)$$

Thus, the optimum location of poles yields the optimum value of POF gain matrix K . In this article, the PSO technique is used for finding the optimum location of poles.

3. LFC Test System Model

The two LFC test system models are considered to demonstrate the performance of the POF-based controller. Firstly, a two-area multiunit multisource hydrothermal power system model used in LFC studies is depicted in Figure 1(a). The detailed modeling of thermal, hydro, and tie-line can be seen in [4]. The second LFC test system, as shown in Figure 1(b), is a two-area multiunit multisource wind-integrated hydrothermal power system model. After incorporating the wind farm system, the overall order of the LFC test system is increased as compared to the first test system.

For performance evaluation, the test LFC system's tie-line power deviation ΔP_{tie12} (in p.u.) is taken into account. By transferring load between different areas, the frequency of generating stations is restored back to the required value. When frequency is controlled by governors followed with the turbine and generator, then that control is called primary control. When the frequency control only by governors is not satisfactory, then secondary control is required. Second level of generation control is called supplementary load frequency control.

The main objective of the multiarea power system is to make the transactions profitable by buying or selling power with neighboring areas. When no power is transmitted through tie lines due to the loss of any generator in a system, then a frequency change is experienced by the units of all the interconnection. Tie lines distribute power networks in consistent units. For maintaining synchronism between tie lines and connected areas, generators are required [4, 5].

4. Control Strategies

4.1. Conventional Lead-Lag-Based Power System Stabilizer (PSS). The PSS is used to give a supplementary control signal in the generator's excitation circuit in order to reduce oscillation. Conventional PSSs are commonly employed in existing power systems to increase the dynamic stability of the power system. Because the power system is significantly nonlinear, the linear model of the power system cannot

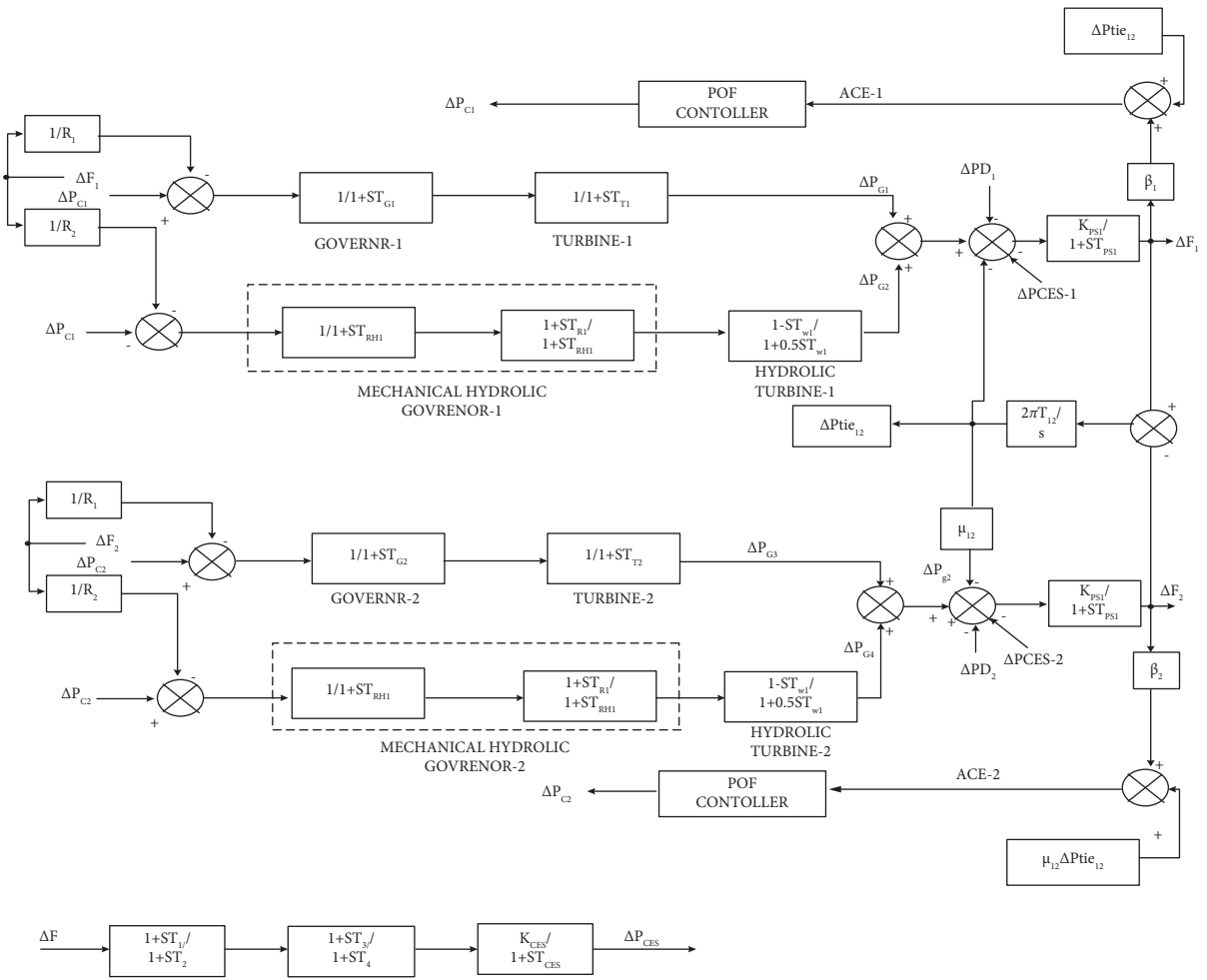


FIGURE 1: Continued.

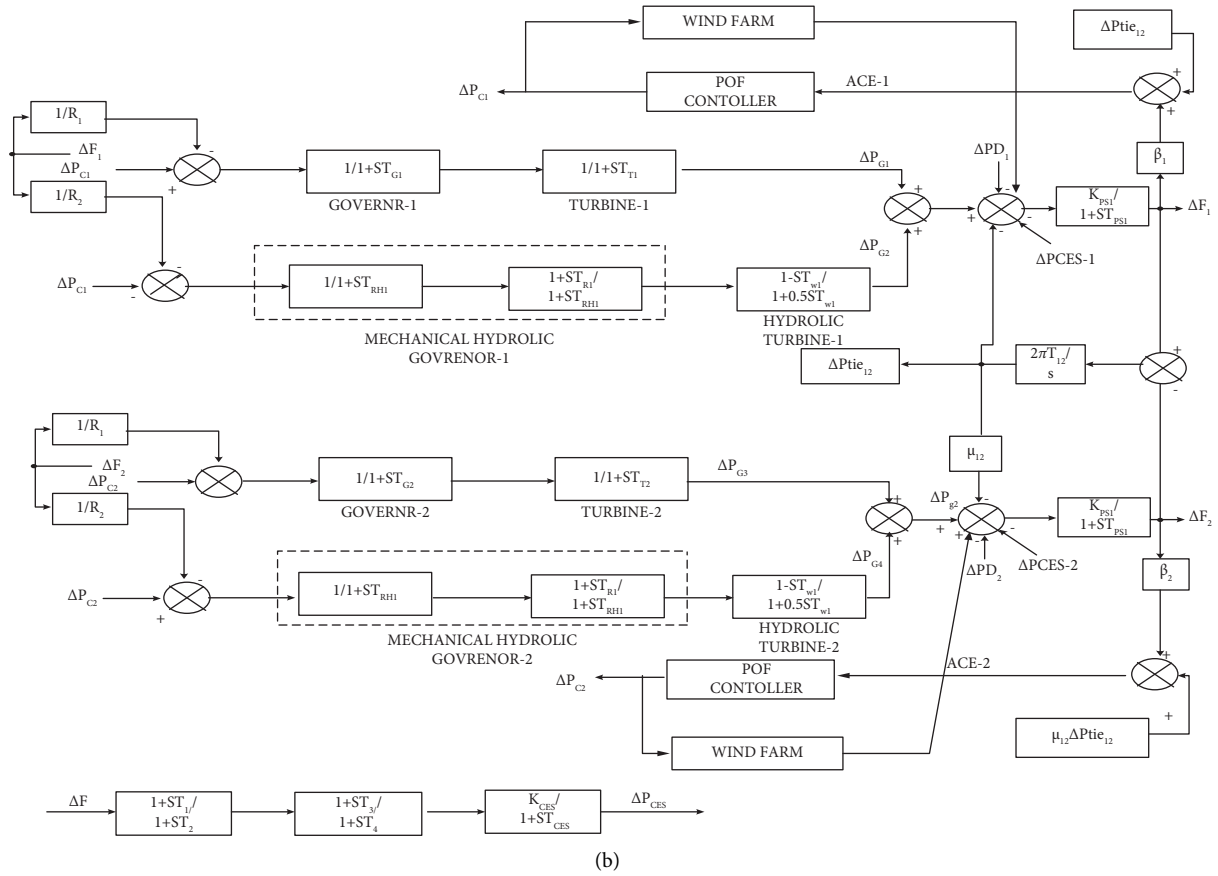


FIGURE 1: (a) The two-area, multisource, multiunit hydrothermal LFC test system model. (b) The two-area, multiunit, multisource wind-integrated hydrothermal power system transfer function model.

assure PSS execution in a practical operational situation. When PSS-based controllers were applied, the settling time and maximum deviation of power system responses were reduced in most cases. PSS controllers resulted in reduced maximum deviations and settling times in some circumstances, but their responses were still significantly smoother and less oscillatory. The neighborhood's conventional PSS (L-PSS), the local PSS plan, uses a linearized model close to an exclusive operating location. The PSS receives the rotor's speed variation as an input. T_w , T_1 , T_2 , and gain K_p are the parameters of the perfect controller that can be constructed with proper tuning. Washout filter, gain, and phase compensation block make up the construction of the lead-lag-based PSS [27].

$$G(s) = K_p \frac{sT_w}{1 + sT_w} \frac{(1 + sT_1)}{(1 + sT_2)} \quad (16)$$

4.2. POF Controller Gain Optimization Using PSO. The gain matrix (K_i) parameters of the POF controller are needed to be optimized for enhanced damping performance of the given LFC system, as compared with the conventional PSS performance. The K_i matrix of the LFC alters the actions of all interconnected machines, affecting each machine's time-domain simulation. As a result, a time-domain simulation-

based goal function is also considered. The integral time square error (ITSE) of angle deviation is used for objective function formulation, as shown.

$$J2 = \sqrt{\sum_{p=1}^x \left(\sum_{i=0}^{T_{ss}} (\Delta\delta_{i,p} - \Delta\delta_{p,initial})^2 \right)}. \quad (17)$$

Here, $\Delta\delta_{p,initial}$ shows the initial angle deviation of the p^{th} generator with respect to the reference machine. The constraints are the upper and lower values of K_i , as shown in (18). This constraint is imposed in order to reduce PSO's search space and save time in determining the best gain matrix value. [28–30] is used as a starting point for the lower and upper bounds of POF gain matrix elements. If the minimum or maximum limit of one or more gain matrix elements approaches, the element's limit is raised by a suitable margin. This is done to get a gain matrix element value that is more close to the optimum value. As a result, the constrained optimization problem can be written as mentioned in (18), while $J2$ should be kept to a minimum level.

$$K_{i,min} \leq K_i \leq K_{i,max} \quad (18)$$

Here, $N = \tau/\Delta$ specifies the totality number of elements in the matrix K_i and i^{th} element is mentioned by K_i .

TABLE 1: Modal analysis without the PSS and with the PSS and POF controller.

Cases	Mode-1		Mode-2		Mode-3	
	Freq. (Hz)	Damp. Factor (δ)	Freq. (Hz)	δ	Freq. (Hz)	δ
Without PSS	0.1281	0.9345	0.2335	0.4643	0.4496	0.1945
PSS	0.1011	0.9613	0.0952	0.8941	0.4135	0.3044
POF	0.0251	0.9874	0.0203	0.9913	0.0033	0.9997

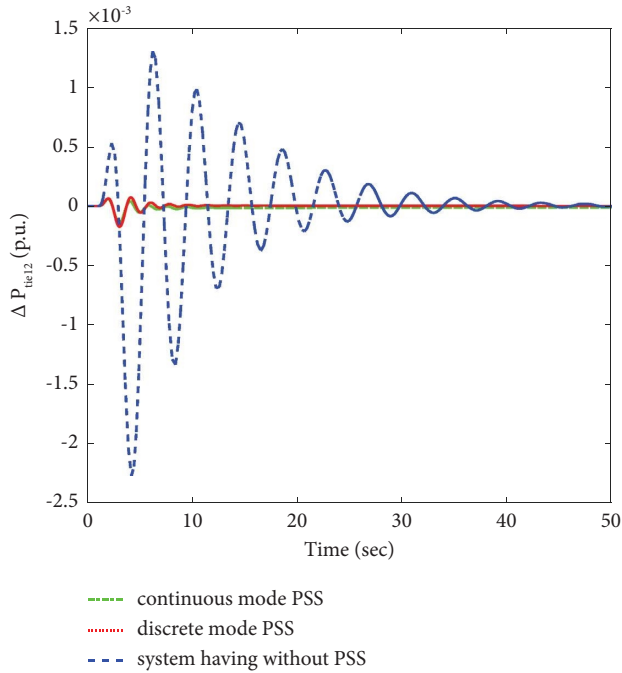


FIGURE 2: Power deviation in tie-line ΔP_{tie12} (p.u.) with respect to time (sec) for without having any PSS, with the continuous PSS, and with the discrete lead-lag-based PSS.

5. Results and Discussion

For the two-area multisource test LFC model, the performance of the LFC system is evaluated using ΔP_{tie12} (in p.u.), where the frequency is held at a nominal value of 60 Hz. For a specific test system, the findings are compared by examining several instances such as without having any PSS, the traditional lead-lag-based PSS, and the POF controller. Table 1 also includes the related modal analysis for the most dominant oscillation modes. The following instances, in particular, are taken into account while evaluating performance.

Case 1. Performance without having any PSS, with the continuous and discrete mode PSS in the LFC system with imperfect medium.

Figure 2 shows the time domain response of P_{tie12} for the evaluation of without any PSS, the continuous and discrete lead-lag-based PSS for the provided LFC system, and with and without PSS consideration. The usual system is adequately damped by the convectional lead-lag based PSS. In the provided LFC system, the convectional PSS performs

well with a perfect medium but fails to dampen oscillations with an imperfect medium.

Figure 3 shows the time domain response of ΔP_{CES1} for the evaluation of without any PSS and the discrete lead-lag-based PSS for the provided LFC system, with and without PSS consideration.

Figure 4 shows the time domain response of ΔP_{g1} for the evaluation of without any PSS and the discrete lead-lag-based PSS for the provided LFC system, with and without PSS consideration.

Figure 5 shows the frequency deviation in area-1 ΔF_1 (p.u.) for the evaluation of without any PSS and the discrete lead-lag-based PSS for the provided LFC system, with and without PSS consideration.

Figure 6 shows the power deviation in area-1 ΔP_{G1} (p.u.) for the evaluation of without any PSS and the discrete lead-lag-based PSS for the provided LFC system, with and without PSS consideration.

Case 2. Performance of the LFC system with the discrete mode PSS, without any noise and the POF controller.

To obtain the optimal performance with the discrete POF controller in the multiarea multisource hydrothermal test LFC system, Δ is varied while keeping the τ constant. The goal is to figure out which input sample interval is best for a specific output sampling period. For the given τ , Table 2 displays the optimal K matrix. Figure 7 presented the tie-line power deviation ΔP_{tie12} (p.u.) with respect to time (sec) with the discrete PSS and POF controller.

Case 3. Performance of the LFC system with the POF controller and switching case.

The system output is sampled at every 0.04 seconds at a given data transportation rate of 25 Hz. Due to sample loss, the output is possibly sampled at 0.08 sec accidentally. A switching system is constructed to display the changeover between these two switching strategies, as shown in Figure 8.

Figure 9 depicts the time domain reaction of the power deviation of two areas while switching from one scheme to another. The controller output sample time interval (Δ) is changed from 0.04 seconds to 0.08 seconds at 2.44 seconds, but if Δ remains at 0.02 seconds, there is a less damping effect on the system's oscillations.

Case 4. Performance of the wind-integrated LFC system with the discrete lead-lag-based PSS and the wind-integrated LFC system with the POF controller ($N=2$, $\tau=0.04$, and $\Delta=0.02$).

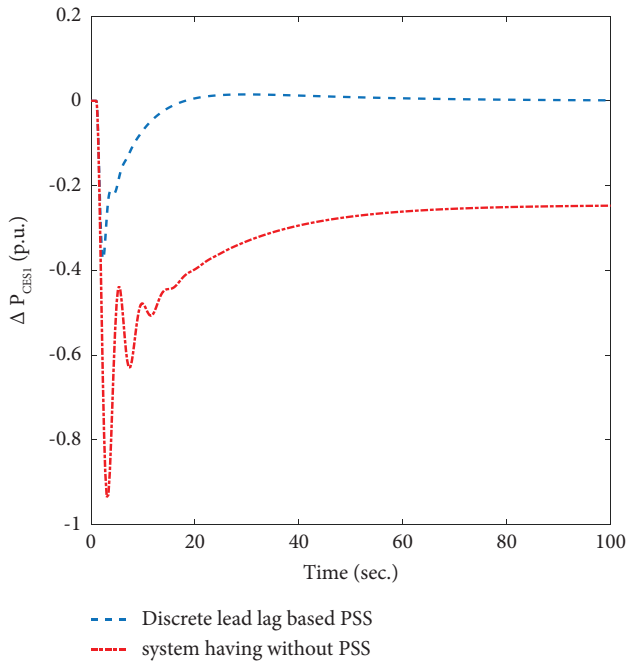


FIGURE 3: Power deviation in capacitive energy storage of area-1 ΔP_{CES1} (p.u.) with respect to time (sec) for without having any PSS and with the discrete lead-lag-based PSS.

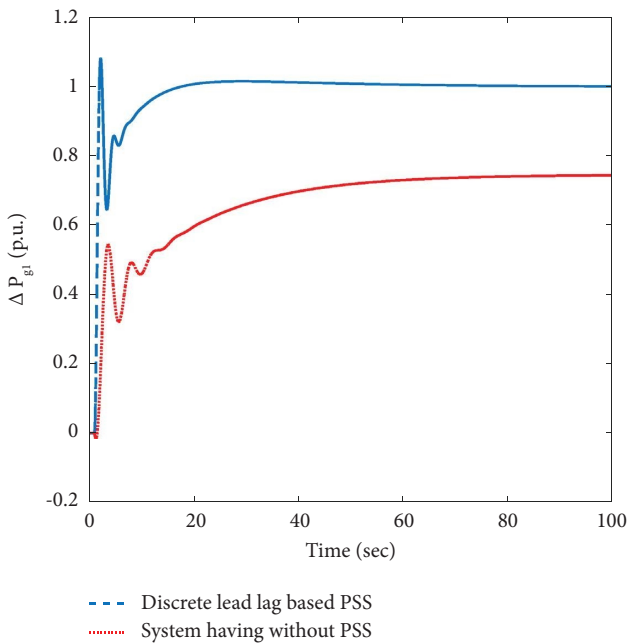


FIGURE 4: Power deviation in generating of area-1 ΔP_{g1} (p.u.) with respect to time (sec) for without having any PSS and with the discrete lead-lag-based PSS.

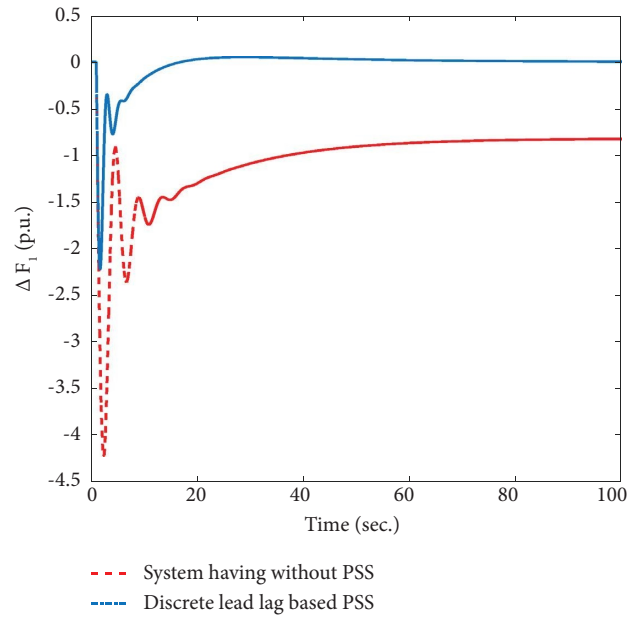


FIGURE 5: Frequency deviation in area-1 ΔF_1 (p.u.) with respect to time (sec) for without having any PSS and with the discrete lead-lag-based PSS.

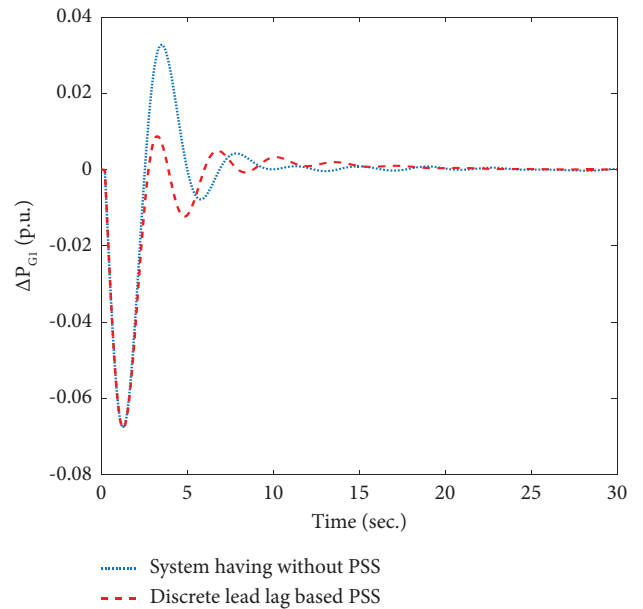


FIGURE 6: Power deviation in governor of area-1 ΔP_{G1} (p.u.) with respect to time (sec) for without having any PSS and with the discrete lead-lag-based PSS.

TABLE 2: Optimal K matrix values for given τ .

N	Δ (sec)	τ (sec)	K
2	0.04	0.08	(0.66101178 -0.82777022)
4	0.02	0.08	(0.661011 -20.997630 30.198576 -2.827770)
5	0.004	0.02	(0.26744 -0.57241 0.95573 -0.61660 0.19186)
10	0.004	0.04	(0.267447 -0.572414 0.719985 -0.720300 0.735929 -0.955737 0.616604 -0.191864 0.657435 -0.477423)

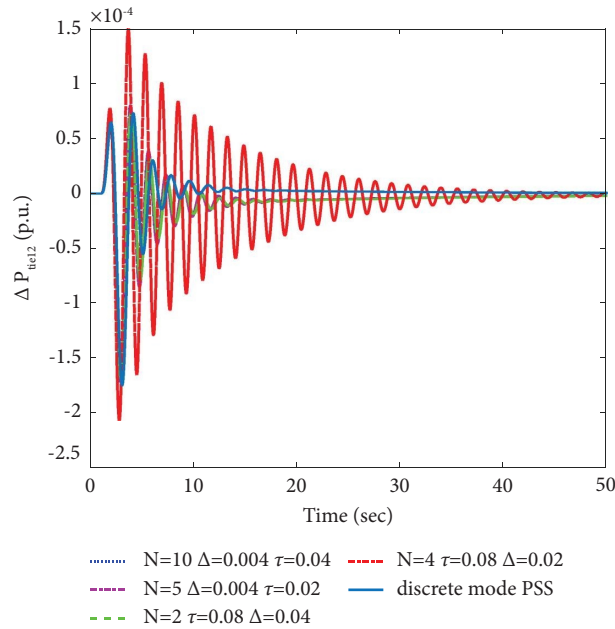


FIGURE 7: Tie line power deviation ΔP_{tie12} (p.u.) with respect to time (sec) with the discrete PSS and POF controller.

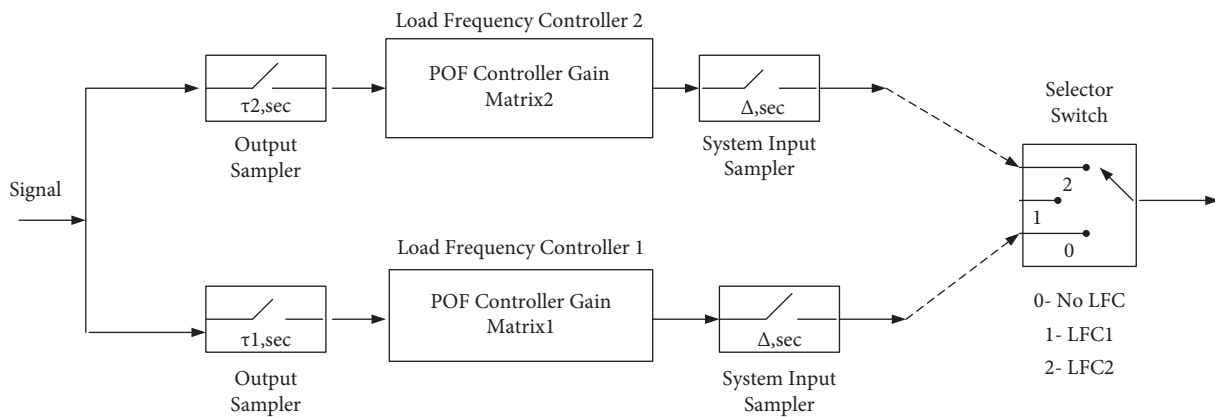


FIGURE 8: The scheme for accidental change in the sampling pattern.

In Figure 10, the time domain response of ΔP_{tie12} is compared with the conventional discrete lead-lag-based PSS and the POF controller having $N=2$, $\tau=0.04$ sec, and

$\Delta=0.02$ sec. The wind-integrated LFC system is also showing better response with the POF controller as compared to the conventional discrete lead-lag-based PSS.

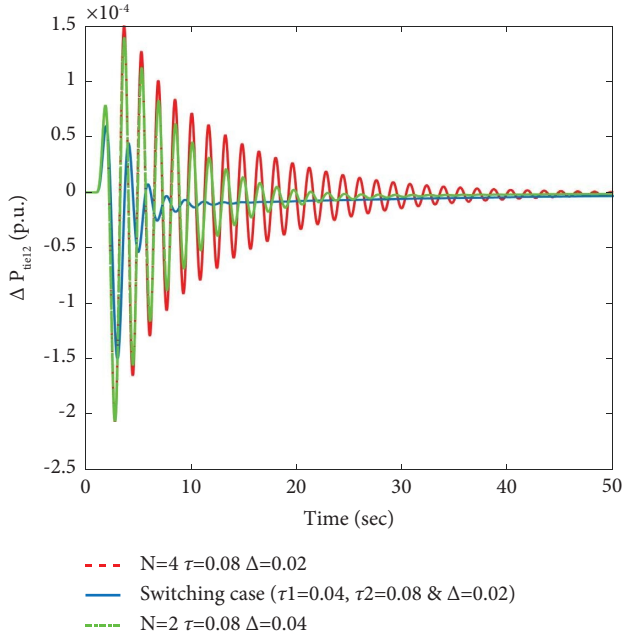


FIGURE 9: Tie line power deviation ΔP_{tie12} (p.u.) with respect to time (sec) with the POF controller having a perfect medium and switching case.

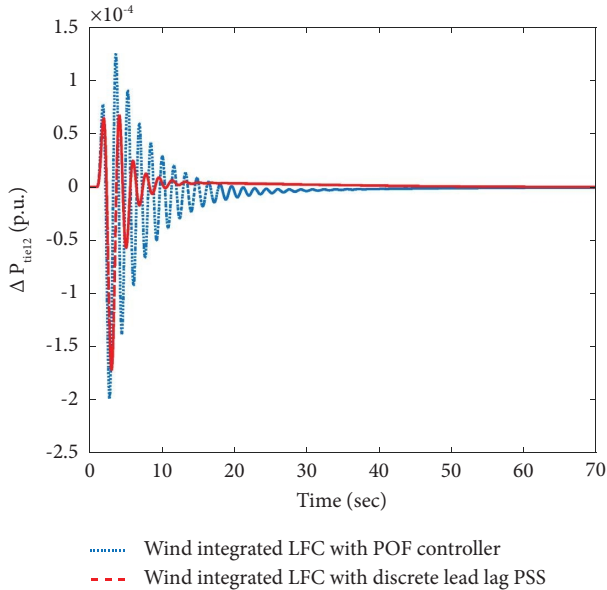


FIGURE 10: Tie line power deviation ΔP_{tie12} (p.u.) with respect to time (sec) for the wind-integrated LFC system having the discrete lead-lag-based PSS and with the POF controller ($N=2$, $\tau=0.04$, and $\Delta=0.02$).

The modal analysis of the given LFC system for three dominant modes of oscillations is shown in Table 1. The value of the damping factor (δ) is increased when the POF-based controller is employed in the given LFC system.

6. Conclusion

A POF-based multiarea multisource hydrothermal LFC system is presented in this study. The POF controller's gain matrix is calculated using the most optimal pole placements and is based on solid theoretical foundations. PSO was used in this study to determine the best pole placement approach, ensuring the stability of the complete LFC system. A numerical modal analysis as well as time domain responses were used to examine the efficiency of the designed POF-based LFC system.

The performance evaluations are made while taking into account the various circumstances from a control standpoint. For time domain analysis, the tie-line power deviation P_{tie12} of the test LFC system with two control zones and hydrothermal coordination is used. The performance analysis takes into account a variety of scenarios, including those without a stabilizer, with a traditional lead-lag based PSS, and with a POF controller. It has been discovered that conventional stabilizers function pretty well with a regular system, with no uncertainties such as transport delay. However, the regular PSS is unable to deal with uncertainties, and as a result, the system as a whole may become unstable. However, strong controllers, such as POF, are capable of dealing with the issue of a faulty communication medium. Table 1 also includes a model analysis corresponding to time domain analysis, which verifies the time domain performance.

Abbreviations

LFC:	Load frequency control
POF:	Periodic output feedback
PSS:	Power system stabilizer
PID:	Proportional integral derivative
PI:	Proportional integral
PSO:	Particle swarm optimization
FOS:	Fast output sampling
CES:	Capacitive energy storage
ACE:	Area control error
ΔF :	Incremental change in area frequency
ΔP_{tie} :	Tie line power deviation
ΔP_G :	Power deviation in governor
ΔP_g :	Power deviation in generating unit
ΔP_{CES} :	Power deviation in capacitive energy storage.

Data Availability

The data supporting the findings of the current study are available from the corresponding author upon request. For the data related queries, kindly contact to Om Prakash Mahela opmahela@gmail.com

Conflicts of Interest

The authors declare that they have no conflicts of interest.

References

- [1] S. Hanwate, Y. V. Hote, and S. Saxena, "Adaptive policy for load frequency control," *IEEE Transactions on Power Systems*, vol. 33, no. 1, pp. 1142–1144, 2018.
- [2] A. Kumar, B. Priya, S. K. Srivastava, H. C. Kumawat, and K. Verma, "Response to the COVID-19: u," *Journal of Policy Modeling*, vol. 43, no. 160, pp. 76–94, 2021, <http://www.gnedenko.net/RTA/index.php/rta/article/view/681>.
- [3] X. Shang-Guana, Y. Hea, and C. Zhang, "Sampled-data based discrete and fast load frequency control for power systems with wind power," *Applied Energy*, vol. 259, pp. 114202–122020, 2020.
- [4] V. Chandrakala, B. Sukumar, and K. Sankaranarayanan, "Load frequency control of multi-source multi-area hydro thermal system using flexible alternating current transmission system devices," *Electric Power Components and Systems*, vol. 42, no. 9, pp. 927–934, 2014.
- [5] J. Talaq and F. Al-Basri, "Adaptive fuzzy gain scheduling for load frequency control," *IEEE Transactions on Power Systems*, vol. 14, no. 1, pp. 145–150, 1999.
- [6] N. Z. Yen and Y. C. Wu, "Optimal periodic control implemented as a generalized sampled-data hold output feedback control," *IEEE Transactions on Automatic Control*, vol. 38, no. 10, pp. 1560–1563, Oct, 1993.
- [7] B. M. Patre and B. Bandyopadhyay, "Periodic output feedback control for two-time-scale discrete systems," in *Proceedings of the IEEE Region 10 International Conference on Global Connectivity in Energy, Computer, Communication and Control (TENCON'98)*, vol. 1, pp. 174–177, New Delhi, India, November 1998.
- [8] M. S. Mahmoud, Y. Chen, and M. Singh, "A two-stage output feedback design," *IEE Proceedings D Control Theory and Applications*, vol. 133, no. 6, pp. 279–284, 1986.
- [9] A. P. Tiwari, B. Bandyopadhyay, and H. Werner, "Spatial control of a large PHWR by piecewise constant periodic output feedback," *IEEE Transactions on Nuclear Science*, vol. 47, no. 2, pp. 389–402, April 2000.
- [10] M. S. Mahmoud and M. G. Singh, "On the use of reduced order models in output feedback design of discrete systems," *Automatica*, vol. 21, no. 4, pp. 485–489, 1985.
- [11] T. H. Li, M. Wang, and Y. Sun, "Dynamic output feedback design for singularly perturbed discrete systems," *IMA Journal of Mathematical Control and Information*, vol. 13, no. 2, pp. 105–115, 1996.
- [12] T. Kaczorek, "Deadbeat control of linear discrete-time systems by periodic output-feedback," *IEEE Transactions on Automatic Control*, vol. 31, no. 12, pp. 1153–1156, 1986.
- [13] T. Kaczorek, "Pole placement for Linear discrete-time systems by periodic output feedbacks," *Systems & Control Letters*, vol. 6, no. 4, pp. 267–269, 1985.
- [14] V. Hernández, "Pole assignment problem for linear discrete-time systems using periodic output-feedbacks," *Proc. 4th Intern. Conf. Sysf. Eng., Coveny, England*, vol. 10-12, pp. 132–135, 1985.
- [15] H. Warner and K. Furuta, "Simultaneous Stabilization based on output measurement," *Kybernetika*, vol. 31, pp. 395–411, 1995.
- [16] B. Bandyopadhyay and C. M. Saaj, "Algorithm on robust sliding mode control for discrete-time system using fast output sampling feedback," *IEE Proceedings - Control Theory and Applications*, vol. 149, no. 6, pp. 497–503, 2002.
- [17] V. Syrmos, C. Abdallah, P. Dorato, and K. Grigoriadis, "Static output feedback A survey," *Automatica*, vol. 33, no. 2, pp. 125–131, 1997.
- [18] H. Werner, "Multimodel robust control by fast output sampling—an LMI approach," *Automatica*, vol. 34, no. 12, pp. 1625–1630, 1998.
- [19] H. Werner and K. Furuta, "Simultaneous stabilization by piecewise constant periodic output feedback," *Control Theory and Technz*, vol. 10, no. 4, pp. 1763–1775, 1995.
- [20] N. Hakimuddin, I. Nasiruddin, T. S. Bhatti, and Y. Arya, "Optimal automatic generation control with hydro, thermal, gas, and wind power plants in 2-area interconnected power system," *Electric Power Components and Systems*, vol. 48, no. 6-7, pp. 558–571, 2020.
- [21] E. Çelik, N. Öztürk, Y. Arya, and C. Ocaç, "(1 + PD)-PID cascade controller design for performance betterment of load frequency control in diverse electric power systems," *Neural Computing & Applications*, vol. 33, no. 22, pp. 15433–15456, 2021.
- [22] K. Peddakapu, M. R. Mohamed, P. Srinivasarao, Y. Arya, P. K. Leung, and D. J. K. Kishore, "A state-of-the-art review on modern and future developments of AGC/LFC of conventional and renewable energy-based power systems," *Renewable Energy Focus*, vol. 43, pp. 146–171, 2022.
- [23] S. Rangi, S. Jain, and Y. Arya, "Utilization of energy storage devices with optimal controller for multi-area hydro-hydro power system under deregulated environment," *Sustainable Energy Technologies and Assessments*, vol. 52, Article ID 102191, 2022.
- [24] G. Sharma, N. Krishnan, Y. Arya, and A. Panwar, "Impact of ultracapacitor and redox flow battery with JAYA optimization for frequency stabilization in linked photovoltaic-thermal system," *International Transactions on Electrical Energy Systems*, vol. 31, no. 5, Article ID e12883, 2021.
- [25] P. S. Rao and I. Sen, "Robust pole placement stabilizer design using linear matrix inequalities," *IEEE Transactions on Power Systems*, vol. 15, no. 1, pp. 313–319, February 2000.
- [26] R. Gupta, A. Kulkarni, and B. Bandyopadhyay, "Power system stabiliser for multimachine power system using robust decentralised periodic output feedback," *IEE Proceedings - Generation, Transmission and Distribution*, vol. 152, no. 1, pp. 3–8, January 2005.
- [27] A. B. Chammas and C. T. Leondes, "Pole assignment by piecewise constant output feedback," *International Journal of Control*, vol. 29, no. 1, pp. 31–38, 1979.
- [28] B. M. Patre, H. Werner, and B. Bandyopadhyay, "Periodic output feedback control for singularly perturbed discrete model of steam power system," *IEE Proceedings - Control Theory and Applications*, vol. 146, no. 3, pp. 247–252, May 1999.
- [29] R. Gupta, B. Bandyopadhyay, and A. M. Kulkarni, "Design of power system stabiliser for single-machine system using robust periodic output feedback controller," *IEE Proceedings - Generation, Transmission and Distribution*, vol. 150, no. 2, pp. 211–216, March 2003.
- [30] P. S. L. Priya and B. Bandyopadhyay, "Periodic output feedback based discrete-time sliding mode control for multivariable systems," in *Proceedings of the IEEE International Conference on Industrial Technology(ICIT)*, col. 19–21, pp. 893–898, Athens, Greece, March 2012.
- [31] M. Bhadu, N. Senroy, and S. Janardhanan, "Discrete wide-area power system damping controller using periodic output

- feedback,” *Electric Power Components and Systems*, vol. 44, no. 17, pp. 1892–1903, 2016.
- [32] S. Wen, X. Yu, Z. Zeng, and J. Wang, “Event-triggering load frequency control for multi area power systems with communication delays,” *IEEE Transactions on Industrial Electronics*, vol. 63, no. 2, pp. 1308–1317, 2016.
- [33] M. Bhadu, “Recommendations of optimal sampling rates for periodic output feedback based discrete mode PS,” *Journal of Engineering. Research EMSME special*, vol. 191, p. 181, 2020.
- [34] H. Werner and K. Furuta, “Simultaneous stabilization based on output measurement,” *Kybernetika*, vol. 31, no. 4, pp. 395–411, 1995.
- [35] G. Dei, “Improved squirrel search algorithm driven cascaded 2DOF-PID-FOI controller for load frequency control of renewable energy based hybrid power system,” in *IEEE Access*, vol. 10, pp. 46372–46391, 2022.
- [36] D. K. Gupta, A. K. Soni, A. V. Jha et al., “Hybrid gravitational–firefly algorithm-based load frequency control for hydrothermal two-area system,” *Mathematics*, vol. 9, no. 7, p. 712, 2021.
- [37] D. K. Gupta, A. V. Jha, B. Appasani, A. Srinivasulu, N. Bizon, and P. Thounthong, “Load frequency control using hybrid intelligent optimization technique for multi-source power systems,” *Energies*, vol. 14, no. 6, p. 1581, 2021.
- [38] A. V. Jha, D. K. Gupta, and B. Appasani, “The PI controllers and its optimal tuning for load frequency control (LFC) of hybrid hydro-thermal power systems,” in *Proceedings of the 2019 International Conference on Communication and Electronics Systems (ICCES)*, pp. 1866–1870, Coimbatore India, July 2019.
- [39] D. K. Gupta, R. Naresh, and A. V. Jha, “Automatic generation control for hybrid hydro-thermal system using soft computing techniques,” in *Proceedings of the 2018 5th IEEE Uttar Pradesh Section International Conference on Electrical, Electronics and Computer Engineering (UPCON)*, pp. 1–6, Gorakhpur, India, November 2018.
- [40] B. Appasani, A. V. Jha, D. K. Gupta, N. Bizon, and A. Srinivasulu, “An improved particle swarm optimization technique and its application in load frequency control,” in *Proceedings of the 2021 13th International Conference on Electronics, Computers and Artificial Intelligence (ECAI)*, pp. 1–5, Pitesti, Romania, July 2021.